

# Rho Meson Propagation and Dilepton Enhancement in Hot Hadronic Matter

R. Rapp<sup>1</sup>, G. Chanfray<sup>2</sup> and J. Wambach<sup>3,4</sup>

1) *Department of Physics, State University of New York, Stony Brook, NY 11794-3800, U.S.A.*

2) *IPN-Lyon, 43 Bd. de 11 Nov. 1918, F-69622 Villeurbanne Cedex, France*

3) *Institut für Kernphysik, TH Darmstadt, Schloßgartenstr.9, D-64289 Darmstadt, Germany*

4) *Department of Physics, University of Illinois, Urbana, IL 61801, U.S.A.*

## Abstract

A realistic model for the free rho meson with coupling to two-pion states is employed to calculate the rho propagator in a hot and dense hadron gas. The medium modifications are based on hadronic rescattering processes: intermediate two-pion states are renormalized through interactions with surrounding nucleons and deltas, and rho meson scattering is considered off nucleons, deltas, pions and kaons. Constraints from gauge invariance as well as the full off-shell dynamics of the interactions are accounted for. Within the vector dominance model we apply the resulting in-medium rho spectral function to compute  $e^+e^-$  production rates from  $\pi^+\pi^-$  annihilation. The calculation of corresponding  $e^+e^-$  spectra as recently measured in central collisions of heavy-ions at CERN/SpS energies gives reasonable agreement with the experimental data.

25.75.+r, 12.40.Vv, 21.65.+f

Typeset using REVTeX

## I. INTRODUCTION

The main objective of ultrarelativistic heavy-ion collisions (URHIC's) is to explore the phase diagram of strongly interacting hadronic matter, in particular possible transitions associated with deconfinement and/or chiral symmetry restoration. Due to its negligible rescattering within the hadronic medium, electromagnetic radiation (photons and dileptons) is believed to be the most suitable probe to study the highest excitation states formed in the early stages of central collisions. In this context, recent measurements of dilepton invariant mass spectra [1–3] in high-energy reactions of protons and sulfur nuclei with heavy target nuclei have raised considerable theoretical discussion. In comparison to the p-A case, central S-A collisions show a strong increase in the dilepton yield (after normalizing to the total number of charged particles). As several hundreds of pions are produced in the sulfur induced reactions, this increase has been attributed to  $\pi^+\pi^- \rightarrow l^+l^-$  annihilation. However, when including this process in numerical transport simulations [4,5] (or hydrodynamical approaches [6,7]) of the collision dynamics, the experimentally observed enhancement in the invariant mass range  $M_{l^+l^-} \simeq 0.3 - 0.6 \text{ GeV}/c^2$  still remains unexplained.

Several mechanisms that might increase the dilepton yield below the  $\rho$  mass have been proposed. In particular, the assumption of a temperature and density dependent dropping  $\rho$  mass [8] as a precursor of the chiral phase transition has been shown to give good agreement with both the CERES and HELIOS-3 dilepton data [4,5]. However, before one can identify this mechanism as an unambiguous signal of (partial) chiral symmetry restoration, the consequences of more 'conventional' scattering processes in the hadronic gas have to be well under control.

In this article we will address this issue, thereby focussing on medium modifications of the  $\rho$  meson that are due to phenomenologically rather well established hadronic interactions. Such processes typically generate a broadening of the  $\rho$  spectral function and therefore also increase the dilepton production at invariant masses below the  $\rho$  mass.

The coupling of the  $\rho$  meson to intermediate 2-pion states in connection with a modified

pion propagation in hot/dense matter has been analyzed *e.g.* in refs. [9–13]. In particular, the interaction of the pions with surrounding nucleons and (thermally excited)  $\Delta$ 's accumulates substantial strength in the  $\rho$  spectral function for invariant masses below 0.6 GeV/c<sup>2</sup>. Further in-medium scattering processes of the  $\rho$  meson have also been shown to work in the same direction, as *e.g.* resonant  $\rho$ -nucleon scattering [14] or interactions with pseudoscalar mesons [15]. We will here extend on our previous analysis [12] by including such processes in a consistent off-shell treatment of  $\rho$  propagation in hot hadronic matter. The inclusion of the proper off-shell dynamics is of particular importance in the low invariant mass region, where the experimentally observed excess of dilepton pairs is most pronounced.

Our article is organized as follows: in the next sect. we first introduce our model for the  $\rho$  meson in free space, which agrees with experimental data on p-wave  $\pi\pi$  scattering and the pion electromagnetic form factor in the relevant (timelike) kinematic regime. We then briefly review the medium modifications of the  $\rho$  meson generated by a renormalization of the pion propagation in a  $\pi N\Delta$  gas as discussed in ref. [11,12]. In the third sect. we turn to the evaluation of in-medium  $\rho$ -baryon scattering. In addition to  $\rho N \rightarrow N(1720), \Delta(1905)$  contributions first discussed by Friman and Pirner [14], we also account for  $\rho$ -like  $NN^{-1}$ ,  $\Delta N^{-1}$ ,  $N\Delta^{-1}$ , and  $\Delta\Delta^{-1}$  excitations. In sect. 4 we calculate the  $\rho$  selfenergy arising from  $\rho\pi$  and  $\rho K/\rho\bar{K}$  scattering. Within the vector dominance model (VDM) the full in-medium  $\rho$  propagator is employed to calculate  $e^+e^-$  production rates in sect. 5. Making use of recent transport results to model the temperature/density evolution of central 200 GeV/u S-Au and 158 GeV/u Pb-Au collisions, and including experimental acceptance, we finally compare our results to the CERES  $e^+e^-$  data.

## II. FREE $\rho$ MESONS AND MEDIUM MODIFICATIONS IN $\pi\pi$ PROPAGATION

## A. The Model for the $\rho$ Propagator in the Vacuum

Our model for  $\rho$  propagator in free space consists of a bare  $\rho$  meson with mass  $m_\rho^{bare}$  renormalized by coupling to intermediate 2-pion states. The basic  $\rho\pi\pi$  interaction vertex is described by the standard form

$$\mathcal{L}_{\rho\pi\pi} = g_{\rho\pi\pi}(\boldsymbol{\pi} \times \partial^\mu \boldsymbol{\pi}) \cdot \boldsymbol{\rho}_\mu, \quad (1)$$

where  $\boldsymbol{\pi}$  and  $\boldsymbol{\rho}_\mu$  denote the isovector pion field and vector-isovector rho meson field, respectively. After resummation of the  $\pi\pi$  bubbles to all orders the scalar part of the  $\rho$  propagator can be cast in the form

$$D_\rho^0(M) = [M^2 - (m_\rho^{bare})^2 - \Sigma_{\rho\pi\pi}^0(M)]^{-1}, \quad (2)$$

which in free space depends on the invariant mass  $M^2 = q_0^2 - \vec{q}^2$  only. The  $\rho$  meson selfenergy due to coupling to 2-pion states is calculated as

$$\begin{aligned} \Sigma_{\rho\pi\pi}^0(M) &= \bar{\Sigma}_{\rho\pi\pi}^0(M) - \bar{\Sigma}_{\rho\pi\pi}^0(0), \\ \bar{\Sigma}_{\rho\pi\pi}^0(M) &= \int \frac{k^2 dk}{(2\pi)^2} v_{\rho\pi\pi}(k)^2 G_{\pi\pi}^0(M, k), \end{aligned} \quad (3)$$

with the vacuum 2-pion propagator

$$G_{\pi\pi}^0(M, k) = \frac{1}{\omega_k^\pi} \frac{1}{M^2 - (2\omega_k^\pi)^2 + i\eta}; \quad \omega_k^\pi = \sqrt{m_\pi^2 + k^2} \quad (4)$$

and the vertex functions

$$v(k) = \sqrt{\frac{2}{3}} g_{\rho\pi\pi} 2k F_{\rho\pi\pi}(k). \quad (5)$$

The hadronic (dipole) form factor

$$F_{\rho\pi\pi}(k) = \left( \frac{2\Lambda_\rho^2 + m_\rho^2}{2\Lambda_\rho^2 + 4\omega_k^2} \right)^2 \quad (6)$$

accounts for the finite size of the  $\rho\pi\pi$  vertex and is normalized to one at the physical resonance energy  $m_\rho=0.77$  GeV. The subtraction of the  $\rho$  selfenergy at zero energy is necessary

to ensure the correct normalization  $F_\pi(0)=1$  for the pion electromagnetic form factor, which in the vector dominance model (VDM) is given by

$$\begin{aligned} |F_\pi^0(M)|^2 &= \frac{(m_\rho^{bare})^4}{(M^2 - (m_\rho^{bare})^2 - \text{Re}\Sigma_\rho^0(M))^2 + (\text{Im}\Sigma_\rho^0(M))^2} \\ &\equiv (m_\rho^{bare})^4 |D_\rho^0(M)|^2 . \end{aligned} \quad (7)$$

Choosing  $g_{\rho\pi\pi}^2/4\pi=2.7$ ,  $\Lambda_\rho=3.1$  GeV and  $m_\rho^{bare}=0.829$  GeV yields a satisfactory description of the vacuum  $\pi\pi$  p-wave scattering phase shifts and the pion electromagnetic form factor in the timelike region (cp. fig. 1).

### B. $\pi\pi$ Propagation in a Hot $\pi N\Delta$ Gas

In general, the  $\rho$  meson propagator in hot/dense matter does not solely depend on invariant mass. Since the notion of temperature specifies a certain rest frame of the heat bath, Lorentz invariance is broken and the vector meson propagator splits into longitudinal and transverse modes (see *e.g.* ref. [17]):

$$D_\rho^{\mu\nu}(q_0, \vec{q}) = \frac{P_L^{\mu\nu}}{M^2 - (m_\rho^{bare})^2 - \Sigma_\rho^L(q_0, \vec{q})} + \frac{P_T^{\mu\nu}}{M^2 - (m_\rho^{bare})^2 - \Sigma_\rho^T(q_0, \vec{q})} + \frac{q^\mu q^\nu}{(m_\rho^{bare})^2 M^2} \quad (8)$$

with the standard projection operators

$$\begin{aligned} P_L^{\mu\nu} &= \frac{q^\mu q^\nu}{M^2} - g^{\mu\nu} - P_T^{\mu\nu} \\ P_T^{\mu\nu} &= \begin{cases} 0 & , \mu = 0 \text{ or } \nu = 0 \\ \delta^{ij} - \frac{q^i q^j}{\vec{q}^2} & , \mu, \nu \in \{1, 2, 3\} \end{cases} . \end{aligned} \quad (9)$$

(the spacelike components of  $\mu$  and  $\nu$  will be denoted by  $i$  and  $j$ , respectively). The longitudinal and transverse selfenergies are defined by the corresponding decomposition of the polarization tensor:

$$\Sigma_\rho^{\mu\nu}(q_0, \vec{q}) = \Sigma_\rho^L(q_0, \vec{q}) P_L^{\mu\nu} + \Sigma_\rho^T(q_0, \vec{q}) P_T^{\mu\nu} . \quad (10)$$

To calculate medium modifications of the  $\rho$  meson which are generated by dressing the intermediate 2-pion states, we adopt the approach of Chanfray and Schuck [11], extended to

finite temperature in ref. [12]. Restricting ourselves to the case of back-to-back kinematics, the  $\rho$  meson selfenergy tensor can be written as

$$\Sigma_{\rho\pi\pi}^{ij}(q_0, \vec{q} = \vec{0}) = \delta^{ij} \Sigma_{\rho\pi\pi}(q_0, \vec{q} = \vec{0}) . \quad (11)$$

Including constraints from gauge invariance the imaginary part of the scalar  $\rho$  selfenergy at given temperature  $T$  and nucleon-delta density  $\rho_{N\Delta} = \rho_N + \rho_\Delta$  takes the form [11]

$$\begin{aligned} \text{Im}\Sigma_{\rho\pi\pi}(q_0, \vec{0}) = & - \int_0^\infty \frac{k^2 dk}{(2\pi)^2} v_{\rho\pi\pi}(k)^2 \int_0^{q_0} \frac{dk_0}{\pi} [1 + f^\pi(k_0) + f^\pi(q_0 - k_0)] \text{Im}D_\pi(q_0 - k_0, k) \\ & * \text{Im}\{\alpha(q_0, k_0, k)D_\pi(k_0, k) + \frac{1}{2k^2}\Pi_L(k_0, k) + \frac{1}{k^2}\Pi_T(k_0, k)\} . \end{aligned} \quad (12)$$

with the longitudinal and transverse spin-isospin response functions

$$\begin{aligned} \Pi_L(k_0, k) &= (k_0^2 - (\omega_k^\pi)^2) \tilde{\Pi}^0(k_0, k) D_L(k_0, k) , \\ \Pi_T(k_0, k) &= (k_0^2 - (\omega_k^\rho)^2) \tilde{\Pi}^0(k_0, k) D_T(k_0, k) , \end{aligned} \quad (13)$$

respectively. The corresponding longitudinal and transverse propagators read

$$\begin{aligned} D_L(k_0, k) &= [k_0^2 - (\omega_k^\pi)^2 - \Sigma_\pi(k_0, k)]^{-1} , \\ D_T(k_0, k) &= [k_0^2 - (\omega_k^\rho)^2 - C_\rho \Sigma_\pi(k_0, k)]^{-1} , \end{aligned} \quad (14)$$

with  $C_\rho=2.2$  and

$$\tilde{\Pi}^0(k_0, k) = \frac{1}{k^2} \Sigma_\pi(k_0, k) , \quad (15)$$

where  $\Sigma_\pi(k_0, k)$  denotes the in-medium single-pion selfenergy, *i.e.*  $D_L$  is equal to the single-pion propagator  $D_\pi$ . The real function  $\alpha$  characterizes corrections to the  $\pi\pi\rho$ -vertex and is related to  $\tilde{\Pi}_R^0(k_0, k) \equiv \text{Re}\tilde{\Pi}^0(k_0, k)$  by

$$\alpha(q_0, k_0, k) = 1 + \tilde{\Pi}_R^0(k_0, k) + \tilde{\Pi}_R^0(q_0 - k_0, k) + \frac{1}{2} \tilde{\Pi}_R^0(k_0, k) \tilde{\Pi}_R^0(q_0 - k_0, k) . \quad (16)$$

The bosefactors  $f^\pi(k_0) = [\exp(k_0/T) - 1]^{-1}$  in eq. (12) account for the thermal occupation of the pions in the intermediate state. The real part of the  $\rho$  selfenergy is obtained from a dispersion integral:

$$\text{Re}\Sigma_{\rho\pi\pi}(q_0) = -\mathcal{P} \int_0^\infty \frac{dE'^2}{\pi} \frac{\text{Im}\Sigma_{\rho\pi\pi}(E')}{q_0^2 - E'^2} \frac{q_0^2}{E'^2} . \quad (17)$$

The factor  $q_0^2/E'^2$  arises from a subtraction at zero energy which ensures gauge invariance in the limit of vanishing three-momentum  $\vec{q}$ .

The single-pion selfenergy  $\Sigma_\pi$  is evaluated within the well-known model of particle-hole excitations [18] extended to finite temperature [19]. Here the pion interacts with surrounding nucleons and thermally excited  $\Delta$ 's through excitations of the type  $NN^{-1}$ ,  $\Delta N^{-1}$ ,  $N\Delta^{-1}$  and  $\Delta\Delta^{-1}$ . The corresponding thermal (retarded) Lindhard function in a given excitation channel  $\alpha=ab^{-1}$ ,  $a,b=N,\Delta$ , reads

$$\phi_\alpha(\omega, k) = - \int \frac{p^2 dp}{(2\pi)^2} f^b(E_p^b) \int_{-1}^{+1} dx \sum_{m=1}^2 \frac{1 - f^a(E_{pk}^a(x))}{\pm\omega + E_p^b - E_{pk}^a(x) \pm \frac{i}{2}(\Gamma_a + \Gamma_b)} \quad (18)$$

including the direct (m=1, signe '+') and the exchange (m=2, signe '-') diagram with

$$\begin{aligned} E_p^{N,\Delta} &= (m_{N,\Delta}^2 + p^2)^{1/2} , \\ E_{pk}^{N,\Delta}(x) &= (m_{N,\Delta}^2 + p^2 + k^2 + 2pkx)^{1/2} . \end{aligned} \quad (19)$$

For the  $\Delta$  width  $\Gamma_\Delta$  we choose a relativistic parametrization given in Ref. [18], but neglect any in-medium width for nucleons, *i.e.*  $\Gamma_N \equiv 0$ . The thermal Fermi distributions,

$$f^a(E_p^a) = (1 + \exp[(E_p^a - \mu_a)/T])^{-1} , \quad (20)$$

determine the nucleon and  $\Delta$  densities at given temperature  $T$  and chemical potential  $\mu_N$ ,  $\mu_\Delta$  to be

$$\begin{aligned} \rho_N(T) &= 4 \int \frac{d^3q}{(2\pi)^3} f^N(E_q^N; \mu_N, T) \\ \rho_\Delta(T) &= 16 \int \frac{d^3q}{(2\pi)^3} f^\Delta(E_q^\Delta; \mu_\Delta, T) . \end{aligned} \quad (21)$$

Throughout this article we will assume chemical equilibrium characterized by a common baryon chemical potential  $\mu_B \equiv \mu_N = \mu_\Delta$  and  $\mu_\pi = 0$ .

From the Lindhard functions one obtains the so-called pionic susceptibilities  $\chi_\alpha^{(0)}$  as [18]

$$\chi_\alpha^{(0)}(\omega, k) = \left( \frac{f_{\pi\alpha} F_{\pi\alpha}(k)}{m_\pi} \right)^2 SI(\alpha) \phi_\alpha(\omega, k) , \quad (22)$$

with spin-isospin factors  $SI(\alpha)$ , a standard monopole form factor

$$F_{\pi\alpha}(k) = \left( \frac{\Lambda_\pi^2 - m_\pi^2}{\Lambda_\pi^2 + k^2} \right) \quad (23)$$

( $\Lambda_\pi=1.2$  GeV) and coupling constants  $f_{\pi\alpha}$  related via  $f_{\pi N\Delta}=2f_{\pi NN}$  (Chew-Low factor [20]) and  $f_{\pi\Delta\Delta}=\frac{1}{5}f_{\pi NN}$  (constituent quark model estimate [21]), cp. table I. For a realistic description of the pion selfenergy the bare susceptibilities have to be corrected for short-range correlation effects between particle and hole. These are parametrized in terms of Migdal parameters  $g'_{\alpha\beta}$ , leading to a system of coupled equations

$$\chi_\alpha = \chi_\alpha^{(0)} - \sum_\beta \chi_\alpha^{(0)} g'_{\alpha\beta} \chi_\beta . \quad (24)$$

It is solved by an elementary matrix inversion with the final result [19]

$$\Sigma_\pi(\omega, k) = -k^2 \sum_\alpha \chi_\alpha(\omega, k) . \quad (25)$$

The Migdal parameters are fixed to  $g'_{\alpha\beta} = 0.8$  for  $\alpha\beta=aa^{-1}bb^{-1}$  and  $g'_{\alpha\beta} = 0.5$  for all others. With the diagonal form eq. (11) of the  $\rho$  selfenergy tensor the corresponding in-medium propagator can be written as

$$D_\rho^{ij}(q_0, \vec{q} = \vec{0}) = \delta^{ij} D_\rho(q_0, \vec{q} = \vec{0}) , \quad (26)$$

where, in analogy to the free case eq. (2), the scalar part is simply

$$D_\rho(q_0, \vec{q} = \vec{0}) = [M^2 - (m_\rho^{bare})^2 - \Sigma_{\rho\pi\pi}(q_0, \vec{q} = \vec{0})]^{-1} . \quad (27)$$

In fig. 2, real and imaginary part of  $D_\rho$  are displayed for different temperatures  $T$  at a fixed baryon chemical potential of  $\mu_N=\mu_\Delta=0.39$  GeV (this value is chosen with respect to what will be used for calculating dilepton spectra in central S-Au collisions in sect. 5). With increasing temperature (which at fixed  $\mu_N, \mu_\Delta$  corresponds to a simultaneous increase in  $\rho_{N\Delta}=\rho_N+\rho_\Delta$ ) we find a strong broadening of the  $\rho$  spectral function. Although the peak



is moderately shifted to higher energies (in accordance with the findings of refs. [9–11]), an appreciable enhancement over the vacuum result is observed for invariant masses below  $M=0.6$  GeV.

In the calculation of  $e^+e^-$  production rates from in-medium  $\pi^+\pi^-$  annihilation (sect. 5) the  $\rho$  spectral function will be weighted with an additional factor of  $1/M^2$  stemming from an intermediate photon propagator. It is instructive to see how this combines with our results for  $\text{Im } D_\rho$  (cp. fig. 3). At highest temperatures the major part of the strength resides in the invariant mass range  $M=0.1\text{--}0.5$  GeV, which simply reflects the softening of the pion dispersion relation: the low-lying  $NN^{-1}$  and  $\Delta\Delta^{-1}$  modes lead to a population of invariant masses around  $M=0.2$  GeV, whereas the  $\Delta N^{-1}$  excitations, strongly washed out by thermal motion and the large  $\Delta$  width, show up at somewhat higher  $M\simeq 0.4$  GeV. In addition, the shift of strength to low invariant masses is accelerated by the appearance of the pion bosefactors in eq. (12). Even at lower densities one clearly recognizes various combinations of pionic branches in the  $1/M^2$ -weighted  $\rho$  spectral function.

To investigate the role that the pionic collectivity plays for the build-up of the medium effects just discussed, we replaced the full propagators  $D_\pi=D_L$  and  $D_T$ , entering eq. (12), by their vacuum forms and recalculated the corresponding  $\rho$  propagator, cp. fig. 4: without the pion collectivity the broadening of the  $\rho$  spectral function is strongly reduced, and the peak is now slightly shifted downwards (short-dashed line). For small temperatures this trend becomes even more pronounced (dotted line). A similar behavior has recently been found in a calculation to lowest order in the nuclear density [22].

### III. RHO SCATTERING IN BARYONIC MATTER

Besides the medium modifications caused by dressing the intermediate 2-pion states, direct interactions of the  $\rho$  meson with surrounding hadrons in the gas have to be considered. In analogy to the in-medium behavior of pions one might expect strong effects from  $\rho$  scattering off baryons (provided their abundance in the hadronic gas is appreciable as seems the

case in central URHIC's at CERN energies [23]). From meson exchange models such as the Bonn potential [24] one certainly knows that *e.g.* the  $\rho NN$  (or  $\rho N\Delta$ ) coupling constant is quite sizeable, even though the corresponding s-channel process  $\rho N \rightarrow N \rightarrow \rho N$  is kinematically strongly disfavored. Such a kinematic suppression will be much less pronounced with increasing energy of the resonance in the intermediate state. Indeed, there are at least two well established resonances in the particle data table [25] which strongly couple to the  $\rho N$  decay channel, namely  $N(1720)$  with isospin/spin-parity  $I(J^P)=\frac{1}{2}(\frac{3}{2}^+)$  and a branching ratio  $\Gamma_{N(1720)\rightarrow\rho N}/\Gamma_{N(1720)}^{tot} > 0.7$ , and  $\Delta(1905)$  with  $I(J^P)=\frac{3}{2}(\frac{5}{2}^+)$ ,  $\Gamma_{\Delta(1905)\rightarrow\rho N}/\Gamma_{\Delta(1905)}^{tot} > 0.6$ . This led Friman and Pirner to the idea [14] of considering  $\rho$ -like particle-hole excitations ('rhosobars') in nuclear matter of the type  $\rho N(1720)N^{-1}$  and  $\rho\Delta(1905)N^{-1}$ . In analogy to the well-known 'pisobar' ( $\pi\Delta N^{-1}$ ), the (non-relativistic) interaction Lagrangian for the two 'rhosobars' can be written as

$$\begin{aligned}\mathcal{L}_{\rho N^* N} &= \frac{f_{\rho N^* N}}{m_\rho} \Psi_{N^*}^\dagger (\vec{S}_{\frac{3}{2}} \times \vec{q}) \cdot (\boldsymbol{\tau} \cdot \vec{\rho}) \Psi_N + h.c. \\ \mathcal{L}_{\rho\Delta^* N} &= \frac{f_{\rho\Delta^* N}}{m_\rho} \Psi_{\Delta^*}^\dagger S_{\frac{5}{2}}^{ij} q^i (\mathbf{T} \cdot \boldsymbol{\rho}^j) \Psi_N + h.c.\end{aligned}\quad (28)$$

( $N^* \equiv N(1720)$ ,  $\Delta^* \equiv \Delta(1905)$ ). Here,  $\vec{S}_{\frac{3}{2}}$  ( $S_{\frac{5}{2}}^{ij}$ ) denote the spin  $\frac{1}{2} \rightarrow \frac{3}{2}$  ( $\frac{5}{2}$ ) transition operator (tensor),  $\boldsymbol{\tau}$ ,  $\mathbf{T}$  the isospin  $\frac{1}{2}$  and the isospin  $\frac{1}{2} \rightarrow \frac{3}{2}$  transition operator, respectively, and  $\vec{q}$  the 3-momentum of the  $\rho$  meson. The coupling constants  $f_{\rho B^* N}$  ( $B^*=N^*$  or  $\Delta^*$ ) are adjusted to reproduce the partial decay widths  $\Gamma_{B^*\rightarrow\rho N}$ . To obtain realistic values for them it is important to account for the finite width of  $\rho$  meson, since both resonances (especially the  $N(1720)$ ) lie rather close to the  $\rho N$  threshold (the assumption of a sharp  $\rho$  meson would allow for only a small phase space, which in turn would result in an overestimate of the coupling constant). Starting from the general expression for the differential two-body decay width, given *e.g.* in ref. [26], we arrive at

$$\Gamma_{B^*\rightarrow\rho N}(\sqrt{s}) = \frac{f_{\rho B^* N}^2}{4\pi m_\rho^2} \frac{2m_N}{\sqrt{s}} \overline{SI}(B^* \rightarrow \rho N) \int_{2m_\pi}^{M_{max}} \frac{MdM}{\pi} A_\rho(M) q_{cm}^3 F_{\rho B^* N}(q_{cm})^2 \quad (29)$$

where  $\overline{SI}(N^* \rightarrow \rho N)=2$ ,  $\overline{SI}(\Delta^* \rightarrow \rho N)=1/3$  are initial-state averaged, final-state summed spin-isospin factors and  $F_{\rho B^* N}(q_{cm})$  is a hadronic monopole form factor ( $\Lambda_{\rho B^* N}=2$  GeV)

depending on the  $\rho/N$  decay 3-momentum in the resonance rest frame,

$$q_{cm}^2 = \frac{(s - M^2 - m_N^2)^2 - 4m_N^2 M^2}{4s} . \quad (30)$$

The  $\rho$  meson spectral function,

$$A_\rho(M) = -2 \text{Im} D_\rho(M) , \quad (31)$$

is taken from eq. (2) and the upper integration limit is  $M_{max} = \sqrt{s} - m_N$ . With a branching ratio of 70% for the  $N(1720)$  decay into  $\rho N$  and a total width of 0.15 GeV at the resonance energy  $m_{N^*} = 1.72$  GeV, eq. (29) determines the coupling to be  $f_{\rho N^* N}^2 / 4\pi = 6.99$ . Applying the same procedure for the  $\Delta(1905)$  with a branching ratio to  $\rho N$  of 60% we find  $f_{\rho \Delta^* N}^2 / 4\pi = 10.64$ .

Having fixed the coupling constant we can now compute the in-medium selfenergy tensors for  $\rho$ -like  $B^* N^{-1}$  excitations from the interaction vertices of eq. (28), leading to

$$\begin{aligned} \Sigma_{\rho N^* N^{-1}}^{(0),ij}(q_0, \vec{q}) &= \left( \frac{f_{\rho N^* N} F_{\rho N^* N}(q)}{m_\rho} \right)^2 IF(\rho N^* N^{-1}) \phi_{\rho N^* N^{-1}}(q_0, \vec{q}) \\ &* \sum_{\lambda_N, \lambda_{N^*}} \langle \frac{3}{2} \lambda_{N^*} | (\vec{S}_{\frac{3}{2}} \times \vec{q})^i | \frac{1}{2} \lambda_N \rangle \langle \frac{1}{2} \lambda_N | (\vec{S}_{\frac{3}{2}}^\dagger \times \vec{q})^j | \frac{3}{2} \lambda_{N^*} \rangle \end{aligned} \quad (32)$$

and a similar expression for the  $\rho \Delta^* N^{-1}$  bubble involving the  $S_{\frac{5}{2}}$  tensor. Both the isospin factors

$$\begin{aligned} IF(\rho N^* N^{-1}) &= 2 \\ IF(\rho \Delta^* N^{-1}) &= \frac{4}{3} \end{aligned} \quad (33)$$

and the Lindhard functions

$$\phi_{\rho\alpha}(q_0, \vec{q}) = - \int \frac{p^2 dp}{(2\pi)^2} f^N(E_p^N) \int_{-1}^{+1} dx \sum_{m=1}^2 \frac{1 - f^{B^*}(E_{pq}^{B^*}(x))}{\pm q_0 + E_p^N - E_{pq}^{B^*}(x) \pm \frac{i}{2} \Gamma_{B^*}^{tot}} \quad (34)$$

( $\alpha = N^* N^{-1}, \Delta^* N^{-1}$ ) are equivalent to the pionic case, eq. (18). The total widths are each taken as the sum of  $\rho N$  channel and  $\pi N$  channel,

$$\Gamma_{B^*}^{tot} = \Gamma_{B^* \rightarrow \rho N} + \Gamma_{B^* \rightarrow \pi N} , \quad (35)$$

where the  $\pi B^* N$  coupling constant is chosen such that the total width matches its experimental value at the resonance mass.

The transversality of the  $\rho N^* N$  coupling automatically ensures that the vector current is conserved, *i.e.*

$$q_i \Sigma_{\rho N^* N-1}^{(0),ij} = 0 , \quad (36)$$

which, when coupling to the photon, is a necessary condition for gauge invariance. Thus, for the  $\Delta(1905)$  contribution we only take into account the transverse part. The corresponding scalar parts of the selfenergy can be extracted by applying the transverse projection operator from eq. (9):

$$\begin{aligned} \Sigma_{\rho\alpha}^{(0)}(q_0, q) &\equiv \frac{1}{2} (P_T)_{\mu\nu} \Sigma_{\rho\alpha}^{(0),ij}(q_0, \vec{q}) \\ &= \frac{1}{2} \left( \frac{f_{\rho\alpha} F_{\rho\alpha}(q)}{m_\rho} \right)^2 SI(\rho\alpha) q^2 \phi_{\rho\alpha}(q_0, q) \\ &\equiv -q^2 \chi_{\rho\alpha}^{(0)}(q_0, q) , \end{aligned} \quad (37)$$

where the spin-isospin factors are summarized in table II. Guided by the experience one has from pion nuclear physics, we also account for short-range correlation effects in the  $\rho$ -like particle-hole bubbles, parametrized by Migdal parameters  $g'$ . The renormalized selfenergy in a given excitation channel then becomes

$$\Sigma_{\rho\alpha}(q_0, q) = -q^2 \frac{\chi_{\rho\alpha}^{(0)}(q_0, q)}{1 + g'_\alpha \chi_{\rho\alpha}^{(0)}(q_0, q)} . \quad (38)$$

For more than one channel one again has to solve a matrix problem as given by eq. (24)

$$\chi_{\rho\alpha} = \chi_{\rho\alpha}^{(0)} - \sum_{\beta} \chi_{\rho\alpha}^{(0)} g'_{\alpha\beta} \chi_{\rho\beta} . \quad (39)$$

Both the  $N(1720)$  and  $\Delta(1905)$  resonances have sufficiently high masses which allow to disentangle their coupling strength to the  $\rho N$  channel through the corresponding decay process. However, within our full off-shell treatment of the in-medium  $\rho$  propagator we are also able to incorporate lower-lying  $\rho$ -like particle-hole excitations. The most obvious candidate is, of course, the  $\Delta(1232)$ : its typical excitation energy of about 300 MeV closely

coincides with the invariant mass region where the experimentally observed excess of dilepton radiation in heavy-ion collisions at CERN energies sets in [1,3]. An appropriate Lagrangian is given by

$$\mathcal{L}_{\rho\Delta N} = \frac{f_{\rho\Delta N}}{m_\rho} \Psi_\Delta^\dagger (\vec{S}_{\frac{3}{2}} \times \vec{q}) \cdot (\mathbf{T} \cdot \vec{\rho}) \Psi_N + h.c. , \quad (40)$$

which automatically includes  $\rho N \Delta^{-1}$  excitations as well. To complete the picture of low-lying  $\rho$ -baryon excitations we furthermore account for  $NN^{-1}$  and  $\Delta\Delta^{-1}$  bubbles described by

$$\begin{aligned} \mathcal{L}_{\rho NN} &= \frac{f_{\rho NN}}{m_\rho} \Psi_N^\dagger (\vec{\sigma} \times \vec{q}) \cdot (\boldsymbol{\tau} \cdot \vec{\rho}) \Psi_N \\ \mathcal{L}_{\rho\Delta\Delta} &= \frac{f_{\rho\Delta\Delta}}{m_\rho} \Psi_\Delta^\dagger (2\vec{\Sigma}_{\frac{3}{2}} \times \vec{q}) \cdot (\boldsymbol{\Theta} \cdot \vec{\rho}) \Psi_\Delta , \end{aligned} \quad (41)$$

where  $\vec{\Sigma}_{\frac{3}{2}}$  and  $\boldsymbol{\Theta}$  denote the spin- $\frac{3}{2}$  and isospin- $\frac{3}{2}$  operators, respectively. The coupling constant  $f_{\rho NN}$  is taken from the Bonn potential, and  $f_{\rho N\Delta}=2f_{\rho NN}$ ,  $f_{\rho\Delta\Delta}=\frac{1}{5}f_{\rho NN}$ , cp. table II. Including Migdal parameters as in the pionic case (all additional ones are uniformly set to  $g'_{\alpha\beta}=0.5$ ), the total selfenergy for  $\rho$ -baryon interactions in the particle-hole picture becomes

$$\Sigma_{\rho BB^{-1}}(q_0, q) = -q^2 \sum_{\alpha} \chi_{\rho\alpha}(q_0, q) \quad (42)$$

where the summation is over  $\alpha = NN^{-1}, \Delta N^{-1}, N\Delta^{-1}, \Delta\Delta^{-1}, N(1720)N^{-1}, \Delta(1905)N^{-1}$ , and the full susceptibilities are determined from solving eq. (39).

In fig. 5 we display the transverse part of the  $\rho$  spectral function,

$$\text{Im}D_\rho^T(M, q) = \text{Im} \left( \frac{1}{M^2 - (m_\rho^{\text{bare}})^2 - \Sigma_{\rho\pi\pi}^0(M) - \Sigma_{\rho BB^{-1}}(q_0, q)} \right) , \quad (43)$$

at fixed baryon chemical potential and with no medium effects included in the 2-pion states. With both increasing density (upper panel in fig. 5) and 3-momentum (lower panel in fig. 5) the 'rhosobar' branches build up an appreciable enhancement for invariant masses below  $M \simeq 0.6$  GeV, together with a depletion of the  $\rho$  peak. However, due to the thermal motion of the nucleons and the relatively large widths of the  $N(1720)$ ,  $\Delta(1905)$  and  $\Delta(1232)$  resonances, the overlapping branch structures are hardly visible; only at the highest nucleon

density considered ( $\rho_N=0.7\rho_0$  at  $T=0.17$  GeV, dotted line in the upper panel of fig. 5) one recognizes a shoulder around  $M=0.6$  GeV corresponding to the  $\rho N^* N$ -channel.

#### IV. RHO SCATTERING IN A THERMAL MESON GAS

In central collisions of heavy nuclei at CERN energies (160-200 GeV/u) large numbers of secondary mesons are produced, clearly exceeding the number of primary nucleons. However, as one knows from the pion, it's properties are typically much less affected in a hot meson gas than in the nuclear medium at comparable densities [27]. Nevertheless, a reliable description of  $\rho$  meson properties at CERN-SpS energies certainly has to account for interactions with surrounding mesons. An analysis of collision rates for (on-shell)  $\rho$ -mesons in a  $\pi/K$  gas has been performed in ref. [15], where a moderate collisional broadening of  $\bar{\Gamma}_\rho^{coll}(T\leq 0.17 \text{ GeV})\leq 60$  MeV has been found.

Our point here is to include  $\rho\pi$  and  $\rho K$  scattering as an additional contribution to the (off-shell)  $\rho$  selfenergy in hot hadronic matter. In analogy to the previous section we assume the dominant contribution to arise from s-channel resonance formation, *i.e.*  $\rho\pi \rightarrow a_1(1260)$  and  $\rho K/\rho\bar{K} \rightarrow K_1(1270)/\bar{K}_1(1270)$ . For the corresponding interaction Lagrangian we choose the one proposed in ref. [28], which is (isospin structure suppressed)

$$\mathcal{L}_{\pi\rho a_1} = G_{\pi\rho a_1} a_\mu (g^{\mu\nu} q \cdot p_\pi - q^\mu p_\pi^\nu) \rho_\nu \pi, \quad (44)$$

being compatible with gauge invariance within the VDM approach.  $a_\mu$ ,  $\rho_\nu$  and  $\pi$  denote the fields for the  $a_1(1260)$  meson, rho meson and pion, and  $q$ ,  $p_\pi$  the rho and pion 4-momenta, respectively. Similarly, we describe the  $K\rho K_1(1270)$  interaction by

$$\mathcal{L}_{K\rho K_1} = G_{K\rho K_1} b_\mu (g^{\mu\nu} q \cdot p_K - q^\mu p_K^\nu) \rho_\nu K \quad (45)$$

( $K$ : kaon field,  $b_\mu$ :  $K_1(1270)$  field). Along the same lines as in the previous section we fix the coupling constants  $G$  by adjusting the partial decay widths  $\Gamma_{a_1\rightarrow\pi\rho}$ ,  $\Gamma_{K_1\rightarrow K\rho}$  to their experimental values. Including the finite width of the  $\rho$  meson one has

$$\Gamma_{a_1 \rightarrow \pi \rho}(\sqrt{s}) = \frac{G_{\pi \rho a_1}^2}{24\pi s} \int_{2m_\pi}^{M_{max}} \frac{M dM}{\pi} A_\rho(M) \\ * q_{cm} \left[ \frac{1}{2}(s - M^2 - m_\pi^2)^2 + M^2(m_\pi^2 + q_{cm}^2) \right] F_{\pi \rho a_1}(q_{cm})^2 \quad (46)$$

with a hadronic dipole form factor  $F_{\pi \rho a_1}(q_{cm})$  ( $\Lambda_{\pi \rho a_1} = 2$  GeV) and  $M_{max} = \sqrt{s} - m_\pi$ . Assuming  $\Gamma_{a_1 \rightarrow \pi \rho}(\sqrt{s} = m_{a_1}) \equiv \Gamma_{a_1}^{tot} = 0.4$  GeV with  $m_{a_1} = 1.23$  GeV yields  $G_{\pi \rho a_1} = 18.7$  GeV<sup>-1</sup>, which is not very different from the value of 14.8 GeV<sup>-1</sup> obtained for a zero-width  $\rho$  meson in ref. [28]. An analogous calculation for the  $K_1$  width, taking  $\Gamma_{K_1 \rightarrow K \rho}(\sqrt{s} = m_{K_1}) = 0.06$  GeV and  $m_{K_1} = 1.27$  GeV [25], gives  $G_{K \rho K_1} = 15.3$  GeV<sup>-1</sup>.

Within the imaginary time (Matsubara) approach the  $\rho$  meson selfenergy tensor arising from interactions with surrounding pions at temperature  $T$  can be calculated as

$$\Sigma_{\rho\pi}^{\mu\nu}(q_0, \vec{q}) = \int \frac{d^3p}{(2\pi)^3} \frac{1}{2\omega_p^\pi} [f^\pi(\omega_p^\pi) - f^{\pi\rho}(\omega_p^\pi + q_0)] M_{\pi\rho}^{\mu\nu}(p_\pi, q) \quad (47)$$

with bosefactors  $f^\pi$ ,  $f^{\pi\rho}$  and the isospin averaged forward scattering amplitude  $M_{\pi\rho}^{\mu\nu}$ . Assuming the latter to be dominated by  $a_1$  resonance formation one derives from eq. (44):

$$M_{\pi\rho a_1}^{\mu\nu}(p_\pi, q) = \frac{(2I_{a_1} + 1)}{(2I_\rho + 1)} G_{\pi\rho a_1}^2 F_{\pi\rho a_1}(q_{cm})^2 \\ * (g^{\mu\kappa} p_\pi \cdot q - p_\pi^\mu q^\kappa) D_{a_1, \kappa\lambda}(k) (g^{\lambda\nu} q \cdot p_\pi - q^\lambda p_\pi^\nu), \quad (48)$$

where the  $a_1$  propagator at 4-momentum  $k \equiv (p_\pi + q)$  is given by

$$D_{a_1, \kappa\lambda}(k) = \frac{(g_{\kappa\lambda} - k_\kappa k_\lambda / m_{a_1}^2)}{s - m_{a_1}^2 + i m_{a_1} \Gamma_{a_1}^{tot}(s)} \quad (49)$$

( $s = k_\lambda k^\lambda$ ). The total  $a_1$  width  $\Gamma_{a_1}^{tot}(s)$  is taken from eq. (46). Using the projection operators defined in eq. (9) we can extract the explicit form of the longitudinal and transverse part of the selfenergy as

$$\Sigma_{\rho\pi a_1}^L(q_0, q) = (P_L)_{\mu\nu} \Sigma_{\rho\pi a_1}^{\mu\nu}(q_0, \vec{q}) \\ = G_{\pi\rho a_1}^2 \int \frac{p^2 dp dx}{(2\pi)^2 2\omega_p^\pi} [f^\pi(\omega_p^\pi) - f^{\pi\rho}(\omega_p^\pi + q_0)] F_{\pi\rho a_1}(q_{cm})^2 \\ * \frac{[\frac{1}{4}(s - M^2 - m_\pi^2)^2 \frac{M^2}{m_{a_1}^2} + \omega_p^{\pi 2} M^2 (1 - \frac{M^2}{m_{a_1}^2}) - \vec{p}^2 M^2 (1 - \frac{M^2}{m_{a_1}^2}) x^2]}{s - m_{a_1}^2 + i m_{a_1} \Gamma_{a_1}^{tot}}$$

$$\begin{aligned}
\Sigma_{\rho\pi a_1}^T(q_0, q) &= \frac{1}{2} (P_T)_{\mu\nu} \Sigma_{\rho\pi a_1}^{\mu\nu}(q_0, \vec{q}) \\
&= \frac{1}{2} G_{\pi\rho a_1}^2 \int \frac{p^2 dp dx}{(2\pi)^2 2\omega_p^\pi} [f^\pi(\omega_p^\pi) - f^{\pi\rho}(\omega_p^\pi + q_0)] F_{\pi\rho a_1}(q_{cm})^2 \\
&\quad \frac{[\frac{1}{2}(s - M^2 - m_\pi^2)^2 \frac{M^2}{m_{a_1}^2} - \vec{p}^2 M^2 (1 - \frac{M^2}{m_{a_1}^2})(1 - x^2)]}{s - m_{a_1}^2 + im_{a_1}\Gamma_{a_1}^{tot}} \tag{50}
\end{aligned}$$

with  $x = \cos\theta$ ,  $\theta = \angle(\vec{p}, \vec{q})$ . Completely analogous expressions are obtained for  $K\rho$  scattering via  $K_1(1270)$  resonance formation (replacing  $\pi \rightarrow K$ ,  $a_1 \rightarrow K_1$ ; note that the isospin averaging factor in eq. (48) changes from 1 to 2/3 and that the total width entering  $D_{K_1}$  is taken to be  $\Gamma_{K_1}^{tot} = 2\Gamma_{K_1 \rightarrow K\rho}$ ; for antikaons one has  $\Sigma_{\rho\bar{K}K_1} = \Sigma_{\rho KK_1}$  as long as  $\mu_{\bar{K}} = \mu_K$ ). The spin-averaged  $\rho$  propagator in a hot  $\pi$ - $K$  gas is then given by

$$\begin{aligned}
D_\rho(M, q) &= \frac{1}{3} [(P_L)_{\mu\nu} + (P_T)_{\mu\nu}] D_\rho^{\mu\nu}(M, \vec{q}) \\
&= \frac{1}{3} [-g_{\mu\nu} + \frac{q_\mu q_\nu}{M^2}] D_\rho^{\mu\nu}(M, \vec{q}) \\
&= \frac{1}{3} \left( \frac{1}{M^2 - (m_\rho^{bare})^2 - \Sigma_{\rho\pi\pi}^0(M) - \Sigma_{\rho\pi a_1}^L(M, q) - 2\Sigma_{\rho KK_1}^L(M, q)} \right. \\
&\quad \left. + \frac{2}{M^2 - (m_\rho^{bare})^2 - \Sigma_{\rho\pi\pi}^0(M) - \Sigma_{\rho\pi a_1}^T(M, q) - 2\Sigma_{\rho KK_1}^T(M, q)} \right), \tag{51}
\end{aligned}$$

the imaginary part of which is shown in fig. 6 for  $\mu_\pi = \mu_K = 0$ . With increasing temperature (upper panel)  $\pi\rho$  and  $K\rho/\bar{K}\rho$  scattering simply lead to a moderate broadening of the spectral function, which is similar to the results of ref. [15]. The impact of a finite 3-momentum is rather small (lower panel of fig. 6).

## V. $e^+e^-$ SPECTRA IN CENTRAL HEAVY-ION COLLISIONS AT CERN/SPS ENERGIES

The general expression for the dilepton production rate  $R = dN_{l+l-}/d^4x$  per unit of 4-momentum  $d^4q$  in a hadronic medium of temperature  $T$  can be written as

$$\frac{dN_{l+l-}}{d^4x d^4q} = L_{\mu\nu}(q) H^{\mu\nu}(q). \tag{52}$$

To lowest order in the electromagnetic coupling  $\alpha = 1/137$  the lepton tensor is given by



$$L_{\mu\nu}(q) = -\frac{\alpha^2}{3\pi^2 M^2} \left( g_{\mu\nu} - \frac{q_\mu q_\nu}{M^2} \right), \quad (53)$$

where we neglected the rest mass of the leptons compared to their individual 3-momenta  $|\vec{p}_+|$ ,  $|\vec{p}_-|$  (in the following we will focus on the  $e^+e^-$  case).  $q = p_+ + p_-$  is the total 4-momentum of the pair in the heat bath.

To calculate the dilepton production rate from the  $\pi^+\pi^- \rightarrow e^+e^-$  annihilation process we employ the phenomenologically well established vector dominance model (VDM). It relates the hadronic part of the electromagnetic current to the third component of the isovector  $\rho$  meson field as

$$J^\mu = \frac{(m_\rho^{bare})^2}{g} \rho_3^\mu, \quad (54)$$

with the universal VDM coupling constant  $g = g_{\rho\pi\pi}$ . As a consequence, the hadronic tensor  $H^{\mu\nu}$  can be expressed in terms of the imaginary part of the retarded  $\rho$  propagator in hot/dense matter:

$$H^{\mu\nu}(q_0, \vec{q}; \mu_B, T) = -f^\rho(q_0; T) \frac{(m_\rho^{bare})^4}{\pi g_{\rho\pi\pi}^2} \text{Im} D_\rho^{\mu\nu}(q_0, \vec{q}; \mu_B, T) \quad (55)$$

( $f^\rho(q_0, T) = (e^{q_0/T} - 1)^{-1}$ ). On account of current conservation,  $q_\mu \text{Im} D_\rho^{\mu\nu} = 0$ , and using the decomposition eq. (8) we arrive at

$$\frac{dN_{\pi^+\pi^- \rightarrow e^+e^-}}{d^4x d^4q} = -\frac{\alpha^2 (m_\rho^{bare})^4}{\pi^3 g_{\rho\pi\pi}^2} \frac{f^\rho(q_0; T)}{M^2} \frac{1}{3} (\text{Im} D_\rho^L(q_0, q; \mu_B, T) + 2 \text{Im} D_\rho^T(q_0, q; \mu_B, T)) \quad (56)$$

with

$$\text{Im} D_\rho^{L,T}(q_0, q; \mu_B, T) = \frac{\text{Im} \Sigma_\rho^{L,T}(q_0, q; \mu_B, T)}{|M^2 - (m_\rho^{bare})^2 - \Sigma_\rho^{L,T}(q_0, q; \mu_B, T)|^2}. \quad (57)$$

The full  $\rho$  meson selfenergy is obtained from combining the results of the three preceding sections, eqs. (12), (17), (42) and (50):

$$\begin{aligned} \Sigma_\rho^L &= \Sigma_{\rho\pi\pi}^L + \Sigma_{\rho\pi a_1}^L + \Sigma_{\rho K K_1}^L + \Sigma_{\rho \bar{K} \bar{K}_1}^L \\ \Sigma_\rho^T &= \Sigma_{\rho\pi\pi}^T + \Sigma_{\rho B B^{-1}}^T + \Sigma_{\rho\pi a_1}^T + \Sigma_{\rho K K_1}^T + \Sigma_{\rho \bar{K} \bar{K}_1}^T. \end{aligned} \quad (58)$$

In fig. 7 we show our final result for the spin averaged  $\rho$  spectral function  $\text{Im } D_\rho \equiv \frac{1}{3}(\text{Im}D_\rho^L + 2\text{Im}D_\rho^T)$ , which does not exhibit any principally new aspects as compared to the analyses in the previous sections.

For calculating  $e^+e^-$  invariant mass spectra as measured in the CERES experiment the differential rate eq. (56) has to be integrated over 3-momentum as well as the space-time history of a central 200 GeV/u S-Au reaction. Therefore we make use of recent transport calculations [5] according to which the corresponding temperature evolution can be well represented by an exponential decrease

$$T(t) = (T^i - T^\infty) e^{-t/\tau} + T^\infty \quad (59)$$

with an initial temperature  $T^i=0.170$  GeV,  $\tau=8$  fm/c and  $T^\infty=0.110$  GeV. The initial baryon density is predicted by RQMD simulations to be  $\rho_B^i \simeq 2.5\rho_0$  [23]. When including the 12 lowest lying baryonic resonances this corresponds to a baryon chemical potential of  $\mu_B=0.39$  GeV, which is slightly lower than the value we employed in [12]. If we furthermore assume chemical equilibrium, *i.e.*  $\mu_B=\text{const}$  and  $\mu_{meson}\equiv 0$ , the time evolution of baryon and meson densities is completely determined by eq. (59). The such obtained baryon density  $\rho_B(t)$ , *e.g.*, turns out to be in good agreement with the transport simulations. After a variable transformation  $q_0 dq_0 = M dM$  and with an isotropic density profile of the hadronic fireball at each stage of the expansion, eq. (56) becomes

$$\begin{aligned} \frac{dN_{\pi^+\pi^-\rightarrow e^+e^-}}{dM d\eta} = N_0 \frac{\alpha^2 (m_\rho^{bare})^4}{\pi^3 g_{\pi\pi\rho}^2 M^2} \int_0^{t_{fo}} dt V(t) \\ * \int d^3q \frac{M}{q_0} f^\rho(q_0; T(t)) \text{Im}D_\rho(M, q; \mu_B, T(t)) A(M, \vec{q}) . \end{aligned} \quad (60)$$

$A(M, \vec{q})$  accounts for the experimental acceptance cuts on the dilepton tracks as applied in the CERES detector (*i.e.*  $p_T > 0.2$  GeV,  $2.1 < \eta < 2.65$  and  $\Theta_{e^+e^-} > 35$  mrad). We here also include it's finite mass resolution by folding our theoretically calculated spectrum with a gaussian

$$G(M, m) = \frac{1}{\sigma(M)\sqrt{2\pi}} \exp\left(-\frac{(m-M)^2}{2\sigma(M)^2}\right), \quad (61)$$

where the width  $\sigma(M)$  is extracted from ref. [2]. The dimensionless normalization constant  $N_0$  is fixed using free  $\rho$  decays by matching our corresponding total ( $M$ -integrated)  $e^+e^-$  yield with the transport results of Li, Ko and Brown [5]. In eq. (60)  $t_{fo}$  denotes the freezeout time of the hadronic fireball. For central S-Au reactions we use  $t_{fo}=10$  fm/c (corresponding to a baryonic freezeout density  $\rho_B(t_{fo})=0.32\rho_0$ ), but our results are rather insensitive with respect to moderate variations in  $t_{fo}$ . The fireball volume  $V(t)$  is determined by the baryon density as

$$V(t) = \frac{N_B}{\rho_B(t)}, \quad (62)$$

where  $N_B$  denotes the number of participating baryons (which can be absorbed in the normalization constant  $N_0$ ).

In fig. 8 we compare the resulting dielectron spectrum, supplemented with contributions from free Dalitz decays ( $\pi_0, \eta \rightarrow \gamma e^+e^-$ ,  $\omega \rightarrow \pi^0 e^+e^-$ ) and free  $\omega \rightarrow e^+e^-$  decays as extracted from ref. [5], with the CERES data from central S-Au collisions at 200 GeV/u. Apparently, the combined medium effects in the  $\rho$  propagation lead to quite reasonable agreement with the experimental spectrum. As was identified in the preceding sections, both the dressing of the intermediate 2-pion states as well as particle-hole-type excitations by the  $\rho$  meson ('rhosobars') constitute the major part of the effect.

We also performed a similar analysis for central Pb-Au collisions at 158 GeV/u. Here, RQMD predicts initial temperatures and baryon densities of  $T^i \simeq 0.180$  GeV and  $\rho_B^i \simeq 4\rho_0$  [23], which corresponds to a baryon chemical potential of  $\mu_B = 0.408$  GeV. Taking  $\tau = 10$  fm/c and  $T^\infty = 0.105$  GeV in eq. (59), the time evolution of temperature and density as found in transport calculations [29] can again be well reproduced. The much larger system size as compared to the S-Au case increases the fireball lifetime substantially. We account for this by choosing a freezeout time of  $t_{fo} = 20$  fm/c corresponding to a freezeout temperature and density of  $T^{fo} = 0.115$  GeV and  $\rho_B(t_{fo}) = 0.18\rho_0$ , respectively. This is somewhat lower than in S-Au collisions, which reflects the fact that the hadronic cooling becomes more efficient with increasing system size. The comparison of the resulting dielectron spectrum with

preliminary data from the CERES/NA45 collaboration confirms our findings for S-Au case: hadronic rescattering in in-medium  $\rho$  propagation seems to resolve the discrepancy between the experimental data and theoretical results based on the free  $\pi^+\pi^-$  annihilation process.

## VI. SUMMARY AND CONCLUSIONS

Starting from a realistic model for the  $\rho$  meson in free space we have studied  $\rho$  propagation in hot hadronic matter and its impact on dilepton production in URHIC's at CERN-SpS energies. Since the free  $\rho$  strongly couples to  $\pi\pi$  states, an important medium effect arises from the modification of the pion propagation: a strong softening of the pion dispersion relation, generated by the coupling to  $\Delta N^{-1}$  as well as low-lying  $NN^{-1}$ ,  $\Delta\Delta^{-1}$  excitations and further weighted by thermal occupation factors in the hot gas, leads to an appreciable enhancement of the  $\rho$  spectral function from zero to about 0.6 GeV in invariant mass. However, as we have shown earlier [12], these modifications do not yet allow for a quantitative description of the CERES data. We furthermore included *direct* interactions of the  $\rho$  within the hot hadronic environment. Corresponding scattering processes off surrounding nucleons, deltas, pions and kaons, were assumed to be dominated by s-channel resonance graphs, which we derived in accordance with constraints from gauge invariance. Within a full off-shell treatment the most notable contributions come from 'rhosobar'-type  $\Delta N^{-1}$ ,  $N(1720)N^{-1}$  and  $\Delta(1905)N^{-1}$  excitations, which result in a further shift of strength to low invariant masses in the  $\rho$  spectral function.  $a_1(1260)$  and  $K_1(1270)$  resonance formation in  $\rho\pi$  and  $\rho K$  scattering turned out to be less significant. Within the VDM we applied our full  $\rho$  propagator to compute  $e^+e^-$  production rates from in-medium  $\pi\pi$  annihilation. These were integrated according to a temperature/density evolution of central S-Au (200 GeV/u) and Pb-Au (158 GeV/u) collisions as found in recent transport calculations, including experimental acceptance conditions. It turns out that the observed enhancement in the CERES data can be accounted for.

One can certainly think of other medium effects in  $\rho$  propagation that are not included in

our present study. Among those are, *e.g.*, finite temperature modifications of the VDM (*i.e.* corrections to the  $\rho\gamma$  vertex), or  $\sigma$ -tadpole graphs [31], which represent the coupling of the  $\rho$  meson to a scalar field generated by the surrounding hadrons. Furthermore, the vector dominance assumption for the nucleonic sector is presumably less accurate than for the pion, which might overestimate the effects of the baryonic medium somewhat (especially for very low invariant masses). However, we do not expect these shortcomings to affect our results in a major, *qualitative* way. Thus, it seems justified to conclude that medium modifications of the  $\rho$  meson arising from hadronic rescattering can essentially explain the low-mass dilepton enhancement as found in recent experiments at the CERN-SpS. After all, the Brown-Rho conjecture of a dropping  $\rho$  mass might in fact be a related phenomenon, *i.e.* in some sense an efficient way to parametrize the shift of strength to low invariant masses in the  $\rho$  spectral function. However, in our dynamical calculation this shift of strength is due to a strong broadening of the resonance, whereas BR-Scaling predicts a downwards shift of the peak caused by a strong scalar mean field in the hadronic medium. Some of this discrepancy might be resolved when including the  $\sigma$  tadpole graph in our framework. Further refinements also require to include a finite  $\vec{q}$ -dependence of the 2-pion selfenergy. Finally, we need to improve our treatment of the URHIC-dynamics; here, a hydrodynamic approach, which accounts for the full off-shell behavior implicit in our dilepton production rate, is mandatory. Work in all these directions is in progress.

## ACKNOWLEDGMENTS

We are grateful for productive conversations with G.E. Brown, A. Drees, J.W. Durso, B. Friman, C.M. Ko, E.V. Shuryak and H. Sorge. We are indebted to G.Q. Li for providing us with the transport results for free meson decays. One of us (RR) acknowledges financial support from the Alexander-von-Humboldt foundation as a Feodor-Lynen fellow. This work is supported in part by the National Science Foundation under Grant No. NSF PHY94-21309 and by the U.S. Department of Energy under Grant No. DE-FG02-88ER40388.

## REFERENCES

- [1] G. Agakichiev *et al.*, CERES collaboration, Phys. Rev. Lett. **75** (1995) 1272;  
P. Wurm for the CERES collaboration, Nucl. Phys. **A590** (1995) 103c;
- [2] A.Drees for the CERES collaboration, in *Proc. of the International Workshop XXIII on Gross Properties of Nuclei and Nuclear Excitations*, Hirschegg 1995, eds. H. Feldmeier and W. Nörenberg, (GSI-Darmstadt 1995), p.151;  
A. Drees and T. Ullrich, CERES Memorandum (1995), unpublished.
- [3] N. Masera for the HELIOS-3 collaboration, Nucl. Phys. **A590** (1995) 93c;  
I. Kralik for the HELIOS-3 collaboration, in *Proc. of the International Workshop XXIII on Gross Properties of Nuclei and Nuclear Excitations*, Hirschegg 1995, eds. H. Feldmeier and W. Nörenberg, (GSI-Darmstadt 1995), p.143.
- [4] W. Cassing, W. Ehehalt and C.M. Ko, Phys. Lett. **B363** (1995) 35.
- [5] G.Q. Li, C.M. Ko and G.E. Brown, Phys. Rev. Lett. **75** (1995) 4007; Nucl. Phys. **A606** (1996) 568.
- [6] C.M. Hung and E.V. Shuryak, preprint SUNY-NTG-96-16 and LANL-preprint archive hep-ph/9608299.
- [7] J. Sollfrank, P. Huovinen, M. Kataja, P.V. Ruuskanen, M. Prakash and R. Venugopalan, preprint SUNY-NTG-96-25 and LANL-preprint archive nucl-th/9607029.
- [8] G.E. Brown and M. Rho, Phys. Rev. Lett **66** (1991) 2720.
- [9] M. Herrmann, B. Friman and W. Nörenberg, Nucl. Phys. **A545** (1992) 267c; Nucl. Phys. **A560** (1993) 411.
- [10] M. Asakawa, C. M. Ko, P. Lévai and X. J. Qiu, Phys. Rev. **C46** (1992) R1159.
- [11] G. Chanfray and P. Schuck, Nucl. Phys. **A545** (1992) 271c; Nucl. Phys. **A555** (1993) 329.

- [12] G. Chanfray, R. Rapp and J. Wambach, Phys. Rev. Lett. **76** (1996) 368.
- [13] C. Song, V. Koch, S.H. Lee and C.M. Ko Phys. Lett. **B366** (1996) 379.
- [14] B. Friman, in *Proc. of Quark Matter '96, Heidelberg (Germany) 1996*, Nucl. Phys. **A**,  
in press;  
B. Friman and H.J. Pirner, LANL-preprint archive nucl-th/9701016, submitted to Nucl.  
Phys. **A**.
- [15] K. Haglin, Nucl. Phys. **A584** (1995) 719; Phys. Rev. **C53** (1996) R2606.
- [16] G.J. Gounaris and J.J. Sakurai, Phys. Rev. Lett. **21** (1968) 244.
- [17] C. Gale and J. Kapusta, Nucl. Phys. **B357** (1991) 65.
- [18] T.E.O. Ericson and W. Weise, *Pions and Nuclei* (Clarendon, Oxford, 1988).
- [19] R. Rapp and J. Wambach, Nucl. Phys. **A573** (1994) 626.
- [20] G.F. Chew and F.E. Low, Phys. Rev. **101** (1956) 1570.
- [21] G.E. Brown and W. Weise, Phys. Rep. **22** (1975) 221.
- [22] F. Klingl and W. Weise, Nucl. Phys. **A606** (1996) 329.
- [23] H. Sorge, Phys. Lett. **B373** (1996) 16.
- [24] R. Machleidt, K. Holinde and C. Elster, Phys. Rep. **149** (1987) 1.
- [25] Particle Data Group, R.M. Barnett *et al.*, Phys. Rev. **D54** (1996) 1.
- [26] C. Itzykson and J.B. Zuber, *Quantum Field Theory* (McGraw Hill, New York, 1980).
- [27] R. Rapp, PhD thesis Bonn 1996, in *Berichte des Forschungszentrums Jülich* 3195  
(Jülich, 1996).
- [28] L. Xiong, E. Shuryak and G.E. Brown, Phys. Rev. **D46** (1992) 3798.
- [29] G.Q. Li, C.M. Ko, G.E. Brown and H. Sorge, Nucl. Phys. **A**, in press.

- [30] Th. Ullrich for the CERES/NA45 collaboration, in *Proc. of Quark Matter '96, Heidelberg (Germany) 1996*, to appear in Nucl. Phys. **A**.
- [31] B. Friman and M. Soyeur, Nucl. Phys. **A600** (1996) 477.



TABLES

TABLE I. *Spin-isospin transition factors and coupling constants for pion induced (longitudinal) p-wave particle-hole excitations in a hot  $N\Delta$  gas.*

$\pi\alpha$	$\pi NN^{-1}$	$\pi\Delta N^{-1}$	$\pi N\Delta^{-1}$	$\pi\Delta\Delta^{-1}$
$SI(\pi\alpha)$	4	16/9	16/9	400
$f_{\pi\alpha}^2/4\pi$	0.081	0.324	0.324	0.00324

TABLE II. *Spin-isospin transition factors and coupling constants for  $\rho$  meson induced (transverse) p-wave particle-hole excitations in a hot  $N\Delta$  gas.*

$\rho\alpha$	$\rho N(1720)N^{-1}$	$\rho\Delta(1905)N^{-1}$	$\rho\Delta N^{-1}$	$\rho N\Delta^{-1}$	$\rho NN^{-1}$	$\rho\Delta\Delta^{-1}$
$SI(\rho\alpha)$	16/3	8/5	32/9	32/9	8	800
$f_{\rho\alpha}^2/4\pi$	6.99	10.64	18.72	18.72	4.68	0.19

## Figure Captions

**Figure 1:** Our fit to the p-wave  $\pi\pi$  scattering phase shifts (upper panel) and the pion electromagnetic form factor in free space (lower panel); the squares in the lower panel correspond to the Gounaris-Sakurai formula [16], which gives an accurate description of the data.

**Figure 2:** Impact of in-medium  $\pi\pi$  states on the  $\rho$  propagator (upper panel: imaginary part, lower panel: real part) at zero 3-momentum in a hot  $\pi N\Delta$  with chemical potentials  $\mu_B \equiv \mu_N = \mu_\Delta = 0.39$  GeV and  $\mu_\pi = 0$ . The chosen temperatures of  $T = 0.170$  GeV (dotted lines),  $T = 0.149$  GeV (short-dashed lines) and  $T = 0.127$  GeV (long-dashed lines) correspond to  $N\Delta$  densities of  $\rho_{N\Delta}/\rho_0 = 1.41$ , 0.63 and 0.32, respectively. The solid lines represent the results in free space.

**Figure 3:** Imaginary part of the  $\rho$  propagator, weighted with a photon propagator  $1/M^2$ , in a hot  $\pi N\Delta$  gas; medium modifications are due to the dressing of the intermediate 2-pion states; line identification as in fig. 2.

**Figure 4:** Imaginary part of the  $\rho$  propagator with in-medium  $\pi\pi$  states at normal nuclear matter density;  
 long-dashed line: full result at  $T = 0.150$  GeV; short-dashed line: without pionic collectivity (as described in the text) at  $T = 0.150$  GeV; dotted line: without pionic collectivity at  $T = 0.050$  GeV; full line: free space.

**Figure 5:** Imaginary part of the in-medium  $\rho$  propagator when accounting for  $\rho N$  and  $\rho\Delta$  scattering in a hot baryon gas at chemical potential  $\mu_B \equiv \mu_N = \mu_\Delta = 0.39$  GeV;  
 upper panel: for fixed 3-momentum  $q = 0.5$  GeV and temperatures  $T = 0.127$  GeV (long-dashed line),  $T = 0.149$  GeV (short-dashed line) and  $T = 0.170$  GeV (dotted line);  
 lower panel: for fixed temperature  $T = 0.149$  GeV and 3-momenta  $q = 0.25$  GeV (long-dashed line),  $q = 0.5$  GeV (short-dashed line) and  $q = 0.75$  GeV (dotted line).

**Figure 6:** Imaginary part of the in-medium  $\rho$  propagator when accounting for  $\rho\pi$  and  $\rho K/\bar{K}$  scattering in a hot meson gas at zero chemical potential;

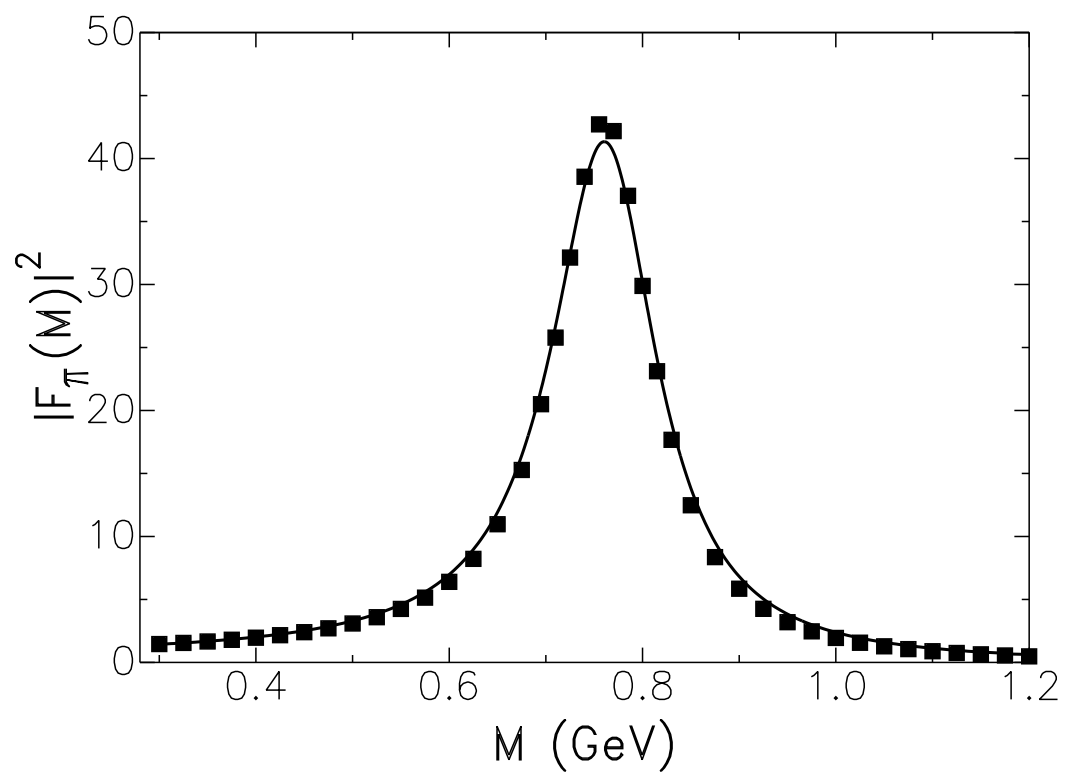
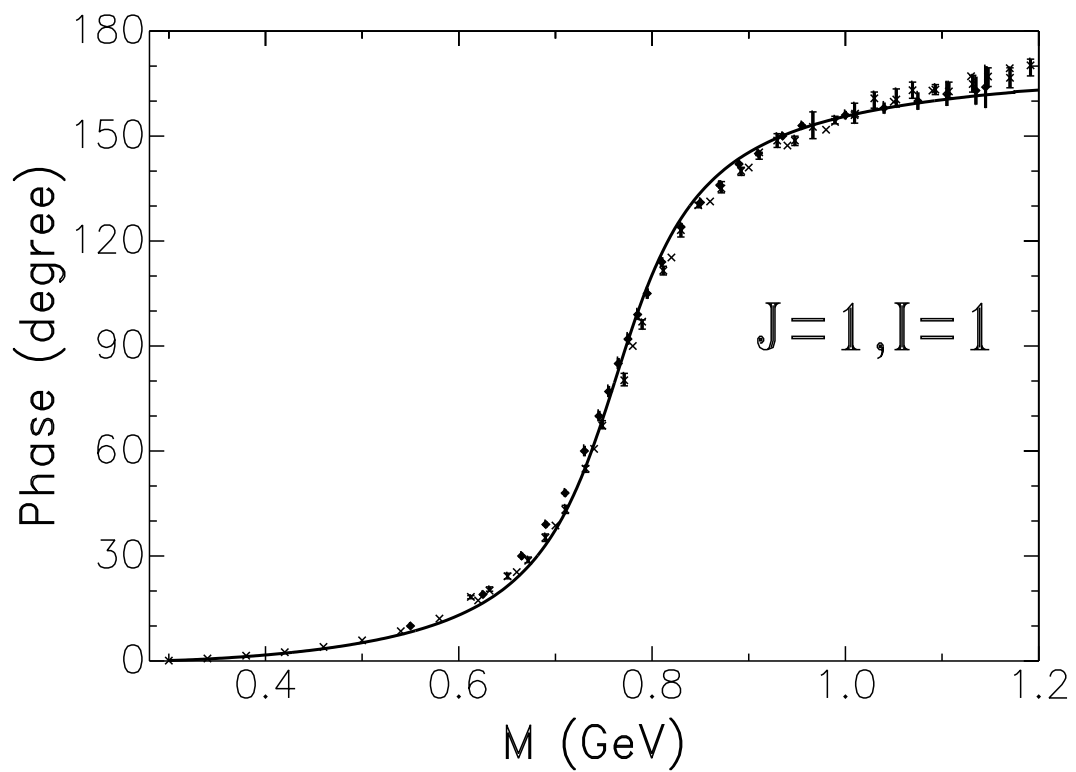
upper panel: for fixed 3-momentum  $q=0.5$  GeV and temperatures  $T=0.127$  GeV (long-dashed line),  $T=0.149$  GeV (short-dashed line) and  $T=0.170$  GeV (dotted line);

lower panel: for fixed temperature  $T=0.149$  GeV and 3-momenta  $q=0$  (long-dashed line),  $q=0.5$  GeV (short-dashed line) and  $q=1$  GeV (dotted line).

**Figure 7:** Our final results for the imaginary part of the in-medium  $\rho$  propagator after inclusion of in-medium  $\pi\pi$  states as well as  $\rho$  meson scattering off nucleons, delta's, pions and (anti-) kaons. The curves correspond to fixed 3-momentum ( $q=0.5$  GeV) and chemical potentials ( $\mu_B=0.39$  GeV,  $\mu_{meson}=0$ ) at temperatures of  $T=0.127$  GeV (long-dashed),  $T=0.149$  GeV (short-dashed) and  $T=0.170$  GeV (dotted).

**Figure 8:** Dielectron spectrum from central S-Au (200 GeV/u) collisions; the dots are the CERES/NA45 data with statistical errors (vertical bars) and systematic uncertainty added independently (resulting in the thick horizontal bars); the dotted curve is the sum of free Dalitz (dashed-dotted line) and  $\omega$  decays (both extracted from recent transport results [5]) as well as free  $\pi^+\pi^-$  annihilation; the full curve is obtained when evaluating the  $\pi^+\pi^-$  contribution with the medium modified  $\rho$  propagator.

**Figure 9:** Same as fig. 8, but for central Pb-Au (158 GeV/u) collisions, where the dots are *preliminary* data from the CERES/NA45 collaboration [30]; here, only the statistical errors are displayed.



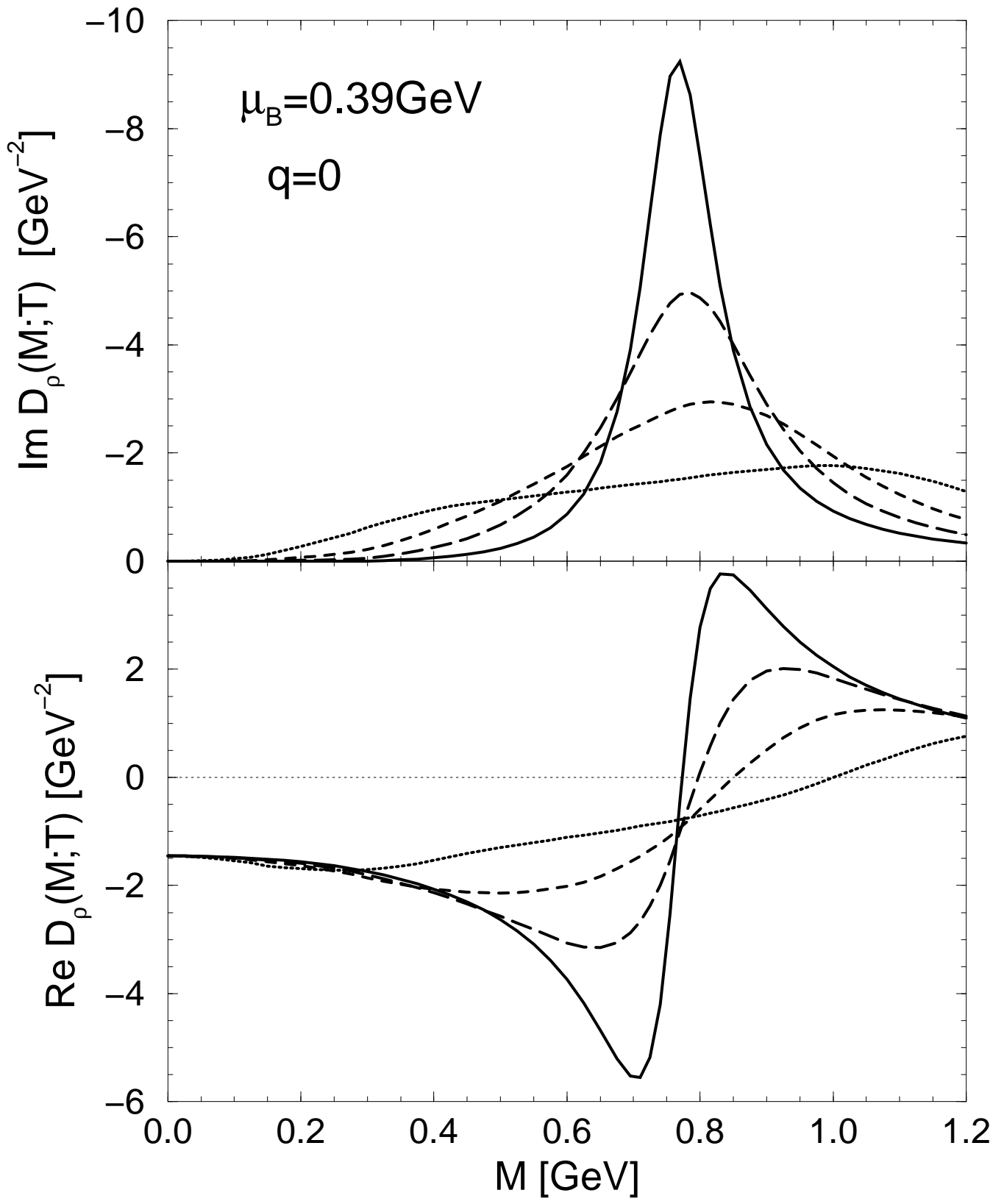


Fig.2

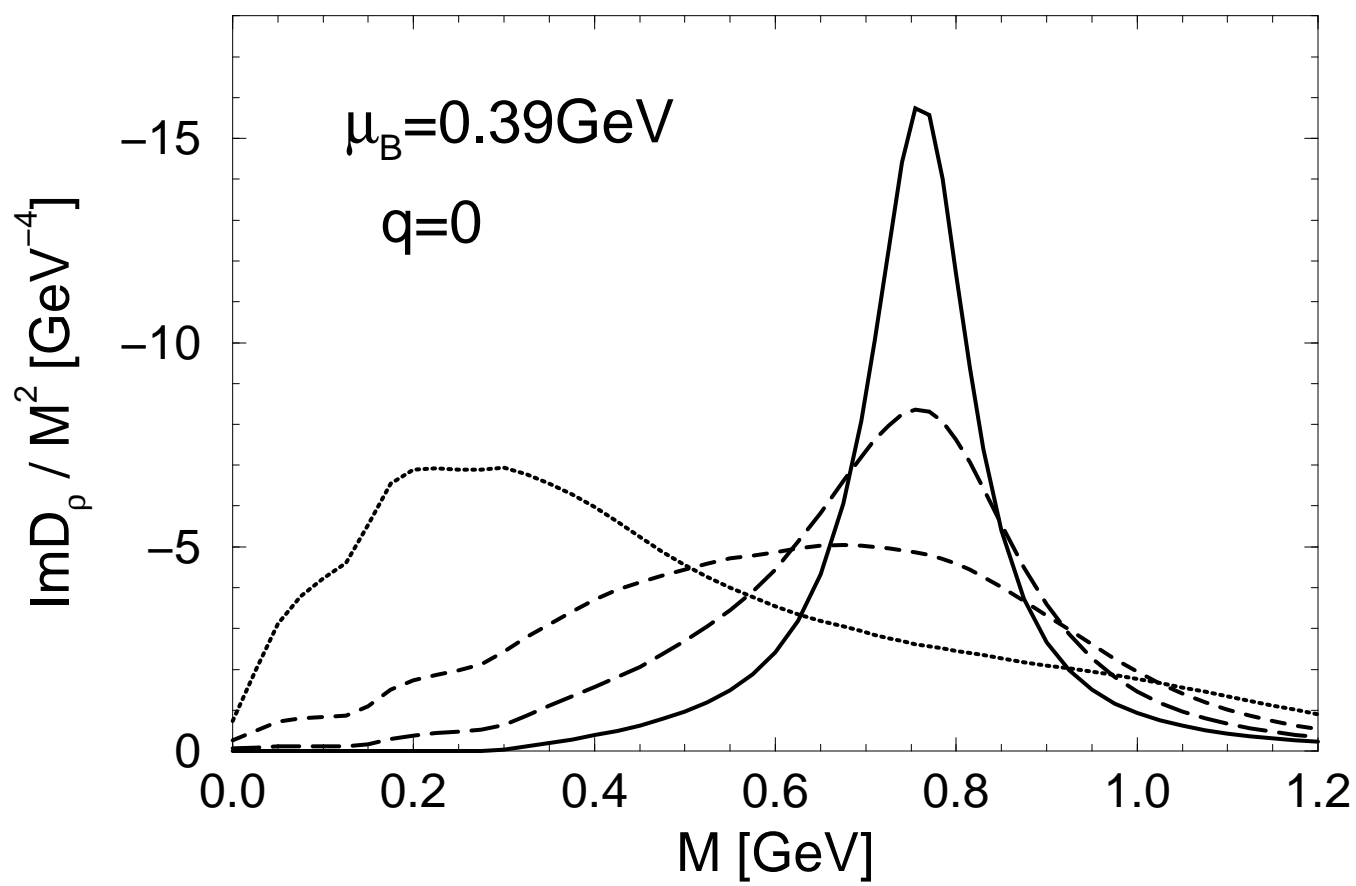


Fig.3

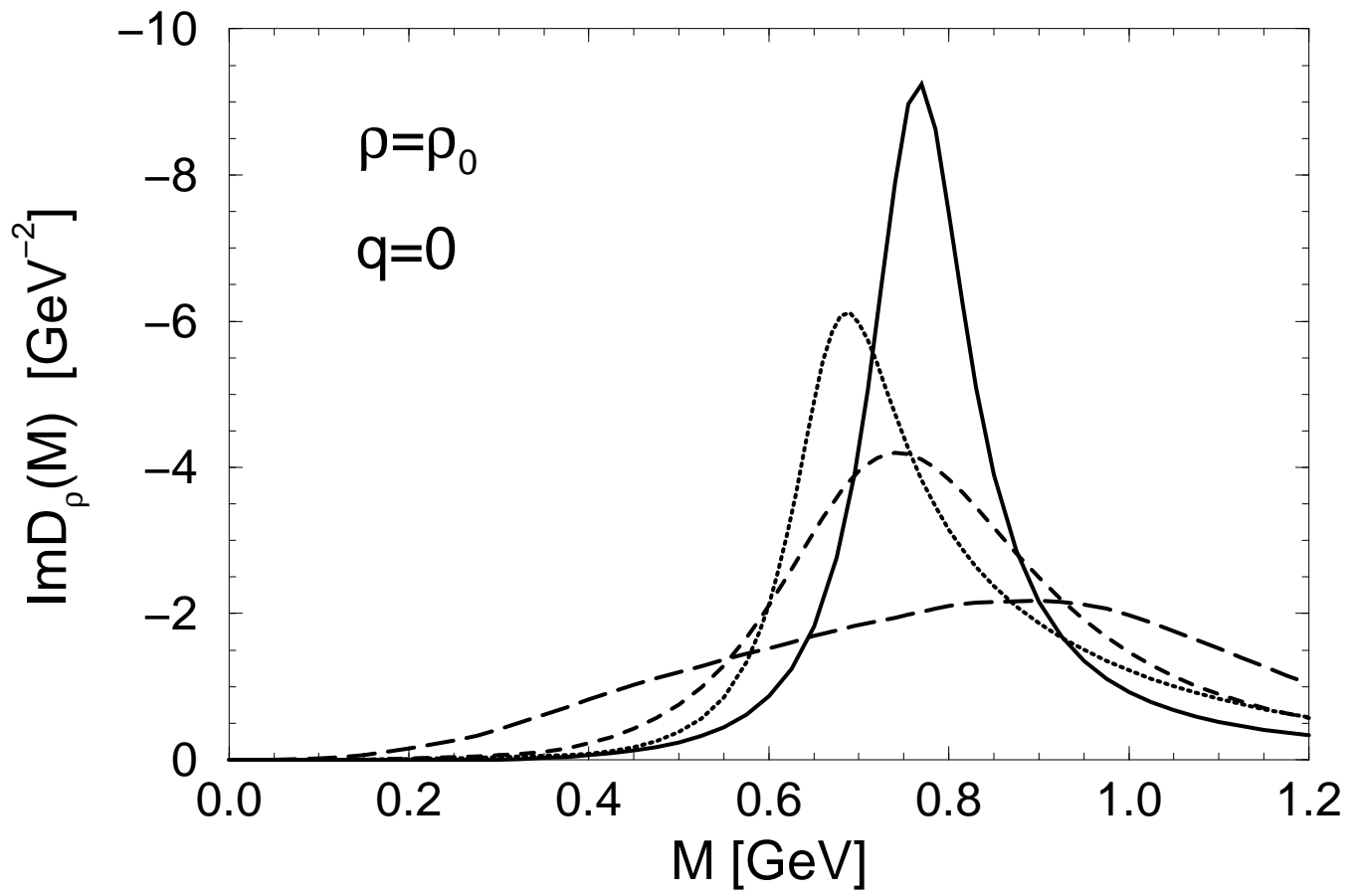


Fig.4

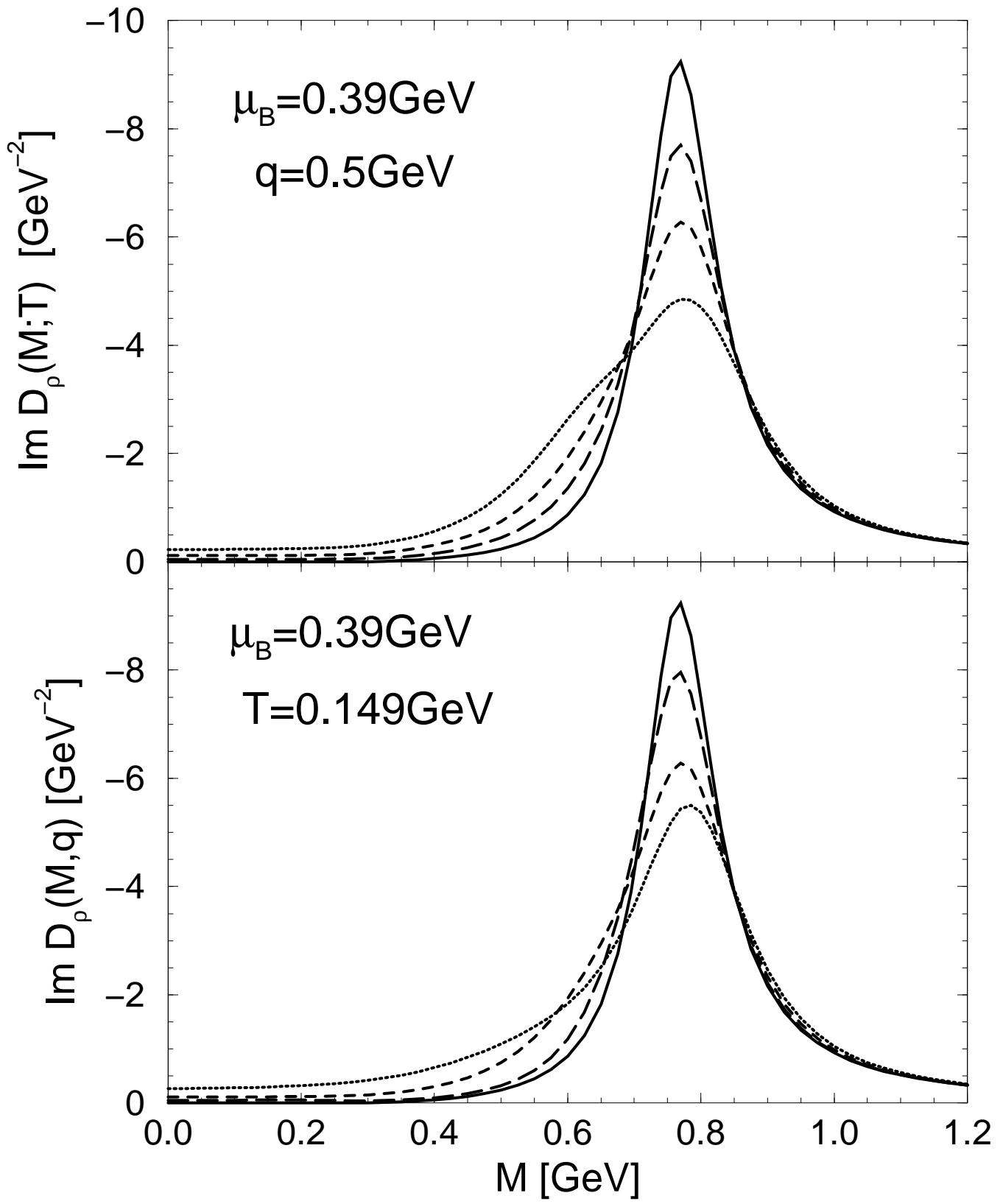


Fig.5



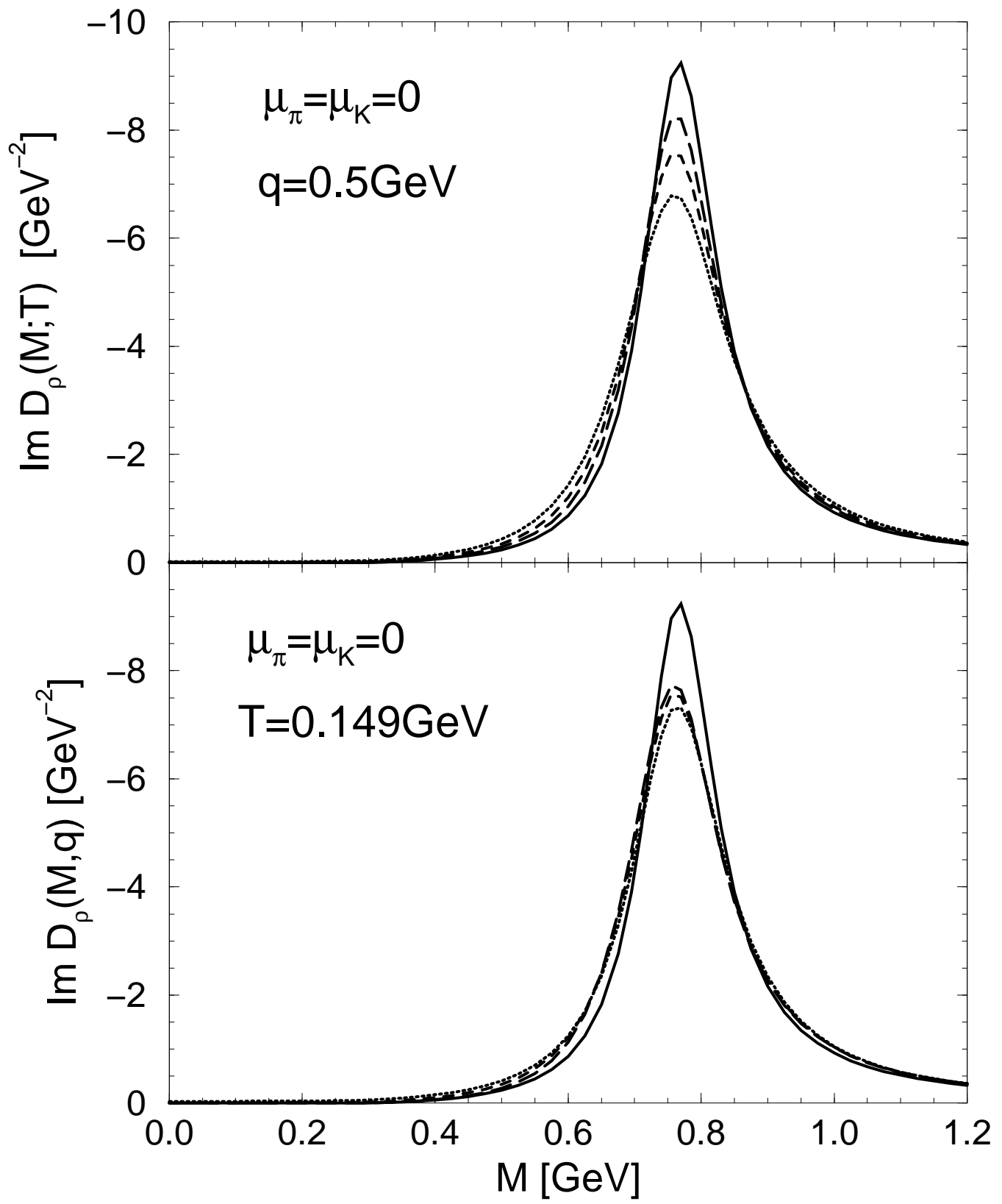


Fig.6

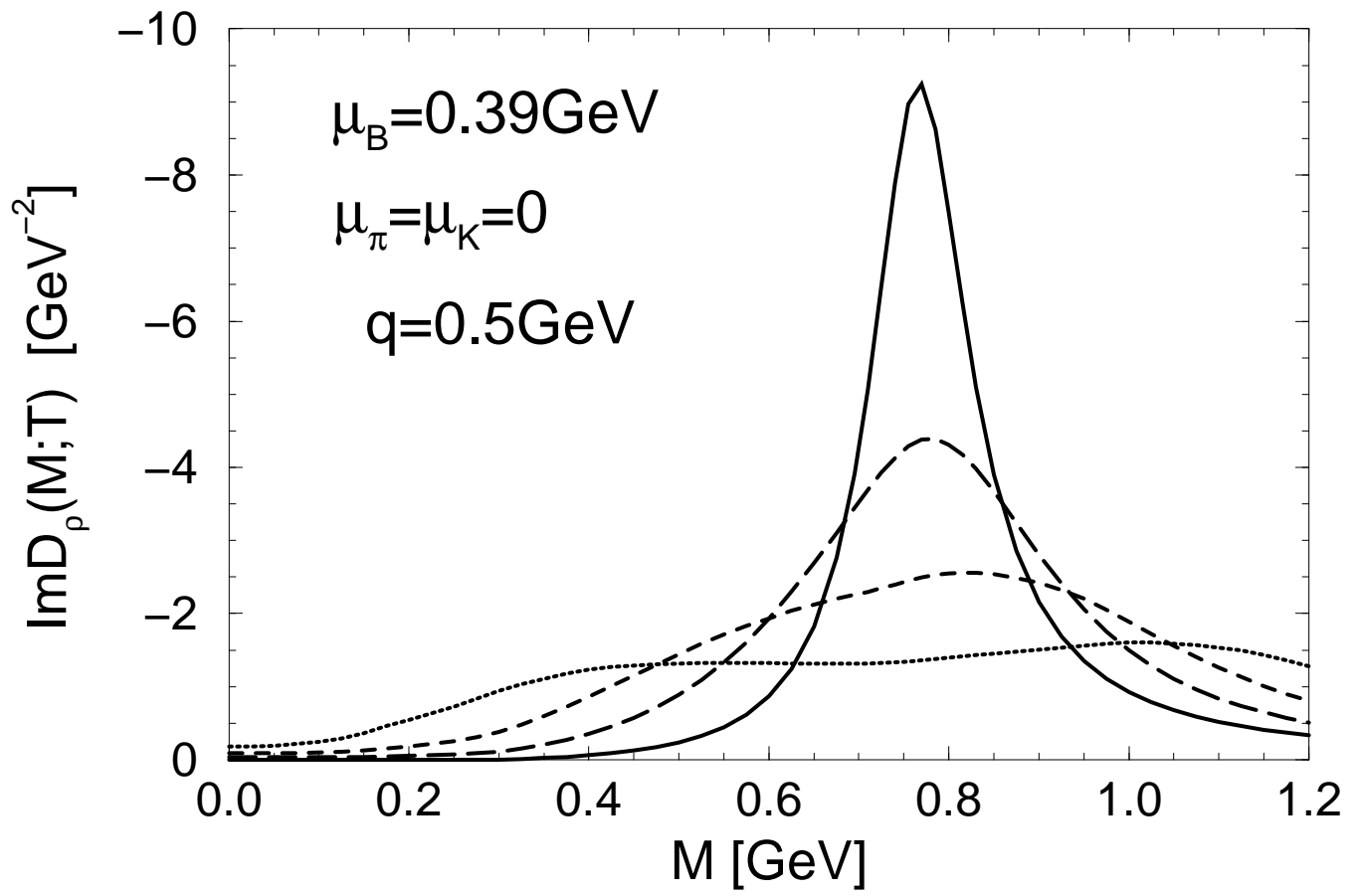


Fig.7

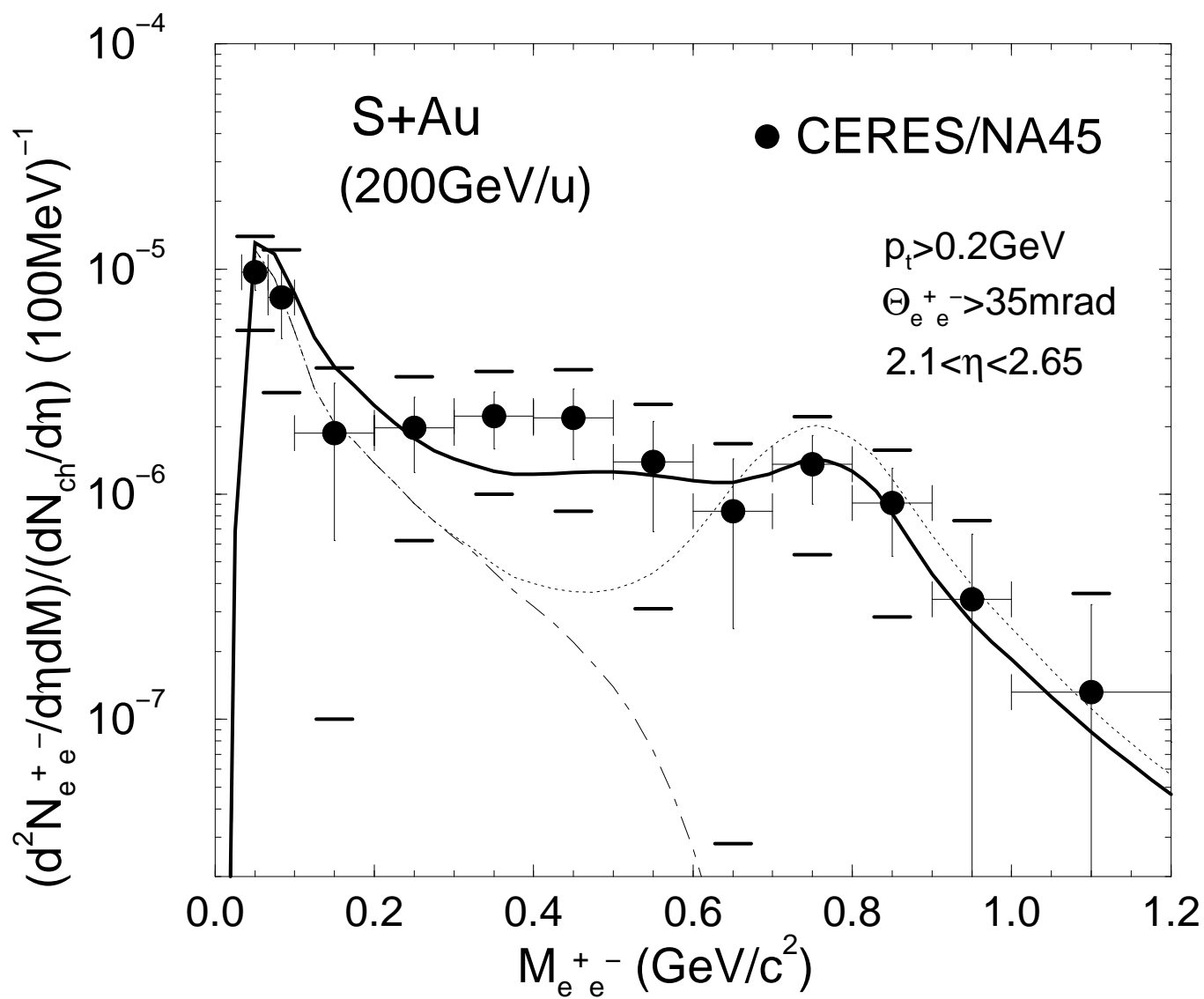


Fig.8

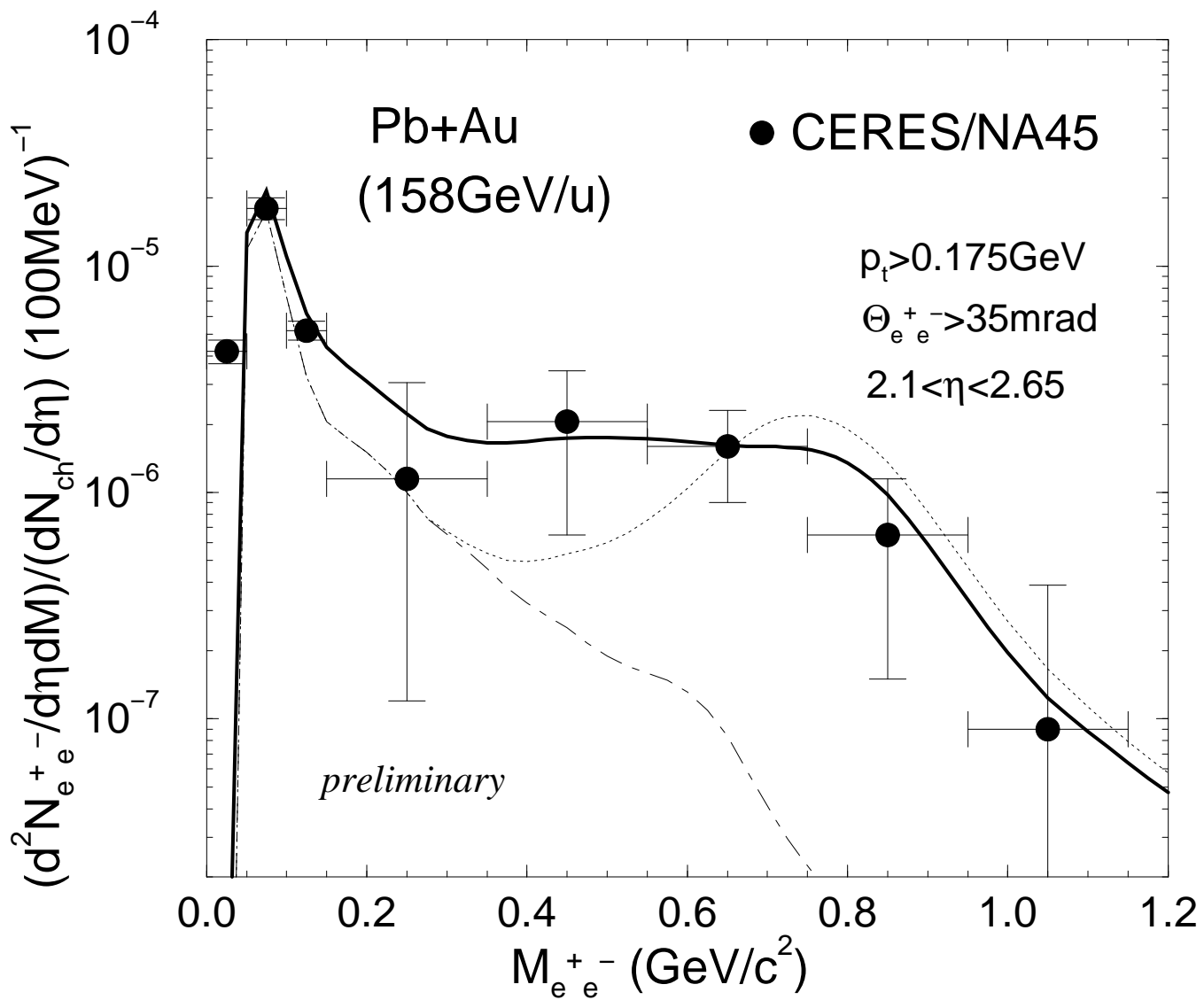


Fig.9